Bioorganic & Medicinal Chemistry 19 (2011) 3265–3273

Contents lists available at ScienceDirect

Bioorganic & Medicinal Chemistry

journal homepage: www.elsevier.com/locate/bmc

Efficient synthesis and chiral separation of ^{11}C-labeled ibuprofen assisted by DMSO for imaging of in vivo behavior of the individual isomers by positron emission tomography

Tatsuya Kikuchi, Maki Okada, Nobuki Nengaki, Kenji Furutsuka, Hidekatsu Wakizaka, Toshimitsu Okamura, Ming-Rong Zhang, Koichi Kato *

Molecular Imaging Center, National Institute of Radiological Sciences, 4-9-1 Anagawa, Inage-ku, Chiba 263-8555, Japan

ARTICLE INFO

Article history:
Received 25 January 2011
Revised 17 March 2011
Accepted 18 March 2011
Available online 27 March 2011

Keywords:
Radiolabeling
Radiolysis
DMSO
Chirality
NSAIDs
Ibuprofen

ABSTRACT

The pharmacological mechanisms focusing on chiral isomer of ibuprofen are not fully understood. Only the (*S*)-isomer of ibuprofen inhibits cyclooxygenases, which mediates the generation of prostanoids and thromboxanes. Consequently, (*S*)-isomers represent a major promoter of the anti-inflammatory effect, and the effects of the (*R*)-isomers have not been widely discussed. However, more recently, the cyclooxygenase-independent pharmacological effects of ibuprofen have been elucidated. Pharmacokinetic studies with individual isomers of ibuprofen by positron emission tomography should aid our understanding of the pharmacological mechanisms of ibuprofen. The efficient ^{11}C-labeling of ibuprofen for chiral separation via the TBAF-promoted α-[^{11}C]methylation was achieved by using DMSO rather than THF as the reaction solvent. The robust production of the radiochemically labile ^{11}C-labeled ibuprofen ester was realized by the protective effect of DMSO on radiolysis. After intravenous injection of each enantiomer of [^{11}C]ibuprofen, significantly high radioactivity was observed in the joints of arthritis mice when compared to the levels observed in normal mice. However, the high accumulation was equivalent between the enantiomers, indicating that ibuprofen is accumulated in the arthritic joints regardless of the expression of cyclooxygenases.

1. Introduction

Non-steroidal anti-inflammatory drugs (NSAIDs) are widely used as therapeutic agents for the treatment of fever, pain and inflammation. NSAIDs are divided into several types based on their chemical structures. Among the different types of NSAIDs, the importance of the chiral center of the arylpropionate type (profens) at the 2-position has been recognized in pharmaceutical sciences. This is because the (*S*)-isomer of these profens possesses an inhibitory effect on cyclooxygenases (COX-1 and/or COX-2) that mediates the generation of prostanoids and thromboxanes.[1,2] Therefore, (*S*)-isomers represent a major promoter of the anti-inflammatory effect, and the effects of the (*R*)-isomers have been essentially overlooked. More recently, the pharmacological effects of NSAIDs that are COX-independent have been elucidated. Anti-tumor activity and the effect towards Alzheimer's disease involve COX-independent pathways,[3] and the (*R*)-isomers of some profens have been found to show a more potent effect than their (*S*)-isomer counterparts.[4] Hamburger and McCay proposed that radical scavenging activities of ibuprofen (**1**) gave an additional anti-inflammatory effect to the COXs inhibition.[5] In addition, Jedlitschky et al. proposed that the inhibition of transmitter storage and release in platelets via multidrug resistance associated protein 4 by NSAIDs may prevent platelet aggregation, besides the inhibition of COXs.[6] Pharmacokinetic studies with individual isomers of profens in conjunction with current knowledge would facilitate further understanding of the pharmacologic effects of NSAIDs and the development of novel NSAIDs.

A significant number of pharmacokinetic studies have been carried out for either racemic or chiral form of **1**; however, there are no reports based on non-invasive in vivo imaging.[7] Positron emission tomography (PET) provides molecular information, such as pharmacokinetics of labeled radiopharmaceuticals and their metabolites.[8] Recently, PET has been considered a useful tool in drug research and development.[9] Direct measurement of in vivo pharmacokinetics by PET can help to advance pharmacological research. Consequently, PET studies of individual stereo-isomers of profens represent an important subject. Since **1** is a representative of profens and shows all the pharmacological activities described

Abbreviations: NSAID, non-steroidal anti-inflammatory drug; COX, cyclooxygenase; PET, positron emission tomography; ee, enantiomeric excess.

* Corresponding author. Tel.: +81 43 206 4041; fax: +81 43 206 3261.
E-mail address: katok@nirs.go.jp (K. Kato).

0968-0896/$ - see front matter © 2011 Elsevier Ltd. All rights reserved.
doi:10.1016/j.bmc.2011.03.041

above, we designed a number of PET studies using chirally enriched **1** labeled with carbon-11. However, there are no reports describing the preparation of ^{11}C-labeled stereo-isomers of **1** ((*R*)-[^{11}C]**1** and (*S*)-[^{11}C]**1**) and the use of these molecules for in vivo PET.[10,11] Thus, individual isomers of ^{11}C-labeled stereo-isomers of **1** were prepared.

Asymmetric synthesis is a well-established research area and versatile methods of enantioselective synthesis of arylpropionate-type NSAIDs including **1** have been developed under non-labeling conditions.[12] However, the time and radioactive constraints of short-lived positron-emitting carbon-11 ($T_{1/2}$ = 20.3 min) restricts the available ^{11}C-labeling agent and reaction operations, thereby limiting the introduction of current methods to produce chiral [^{11}C]**1**. Asymmetric ^{14}C-labeling synthesis of (*R*)-[^{14}C]**1** was reported by Zhang et al.[13] Enantioselective α-[^{14}C]methylation using iodo[^{14}C]methane to a 4-methyl-5phenyl-2-oxazolidinone imide derivative was the key step of this synthesis and (*R*)-[^{14}C]**1** was obtained in 47% overall yield with more than 98% enantiomeric excess (ee). Although iodo[^{14}C]methane in the synthetic scheme could be replaced by iodo[^{11}C]methane (**2**) formally, a longer reaction time at low temperature for α-[^{14}C]methylation and isolation before the removal of the chiral auxiliary would be difficult to translate for the synthetic labeling of short-lived carbon-11.

Chiral separation by high-performance liquid chromatography (HPLC) is a useful strategy for the preparation of both enantiomers, and the molar scale of ^{11}C-labeling is suitable for a semi-preparative HPLC approach.[14] Each PET tracer should be synthesized for every PET experiment. This is because of the short-lived radioactive character of the PET tracer. Therefore, this feature can offset the disadvantage of chiral separation by HPLC where only less than half of the product is usable. However, there are additional aspects required before introducing this technology into PET tracer synthesis as compared with non-labeling syntheses. Usually, normal-phase HPLC is used for the separation of versatile chiral molecules. Conversely, reversed-phase HPLC is preferable for the separation step of PET tracer syntheses by semi-preparative HPLC. In addition, the isolated fraction should be administered to animals or humans after evaporation, and this condition limits the usable buffer systems. As a result, chiral separation has not frequently been introduced into PET tracer syntheses.[15]

Hence the radioactivity of each chiral product should be less than half following chiral separation, and efficient production of racemic [^{11}C]**1** was necessary. Consequently, a method which yields racemic [^{11}C]**1** with high efficiency from the starting ^{11}C-labeling agent was needed. We recently developed the synthesis of [^{11}C]**1** via TBAF-promoted α-[^{11}C]methylation of methyl (4-isobutylphenyl)acetate (**3**) using **2** in THF with high total radiochemical conversion (Scheme 1).[11] The remote-controlled synthesis, which is crucial for efficient production, was successful for this method. We considered that the first step toward the chiral separation of [^{11}C]**1** was solved. However, radiolysis of ^{11}C-labeled products with high radioactivity and high specific activity is an additional problem.[16] Takashima-Hirano et al. reported that ^{11}C-labeled methyl ester analogs of some profens were radiolysis labile under the high radioactivity level and the rank of ^{11}C-labeled ibuprofen methyl ester ([^{11}C]**4**) was the highest by their criteria.[10] Although the method for the α-[^{11}C]methylation of **3** was different, a similar issue was considered in our case. It was unclear how much radiolysis of [^{11}C]**4** influenced the isolated radioactivity of the final products and it should appear en route to the preparation of racemic [^{11}C]**1** during our multi-step synthesis. A treatment that would suppress the radiolysis of [^{11}C]**4** without influencing the entire (*R*)- or (*S*)-[^{11}C]**1** synthesis was necessary. We proposed the suppression of radiolysis using the solvent effect. Here, we described the successful efficient production of racemic [^{11}C]**1** via TBAF-mediated α-[^{11}C]methylation and chiral separation of both enantiomers of [^{11}C]**1** by chiral HPLC with a reversed stationary phase. Remarkable solvent effects, which were obtained by the replacement of THF with DMSO, are also described. In addition, we present preliminary results showing the accumulation of the individual stereo-isomers of [^{11}C]**1** in the joints of arthritis mice measured by PET.

2. Material and methods

2.1. Chemicals

(4-Isobutylphenyl)acetic acid was purchased from Toronto Research Chemicals Inc. (North York, ON, Canada) via WAKO Pure Chemical Industries Ltd (Osaka, Japan). (*S*)- and (*R*)-**1** were purchased from Tokyo Chemical Industry Ltd (Tokyo, Japan) and Enzo Life Science International Inc. (Plymouth Meeting, PA, USA), respectively. Ibuprofen, tetrabutylammonium bifluoride, 1.0 M solution of TBAF in THF and DBU were purchased from Tokyo Chemical Industry Ltd (Tokyo, Japan). Methyl phenylacetate (**5**), triethylamine and 2-phenyl-propanoic acid were purchased from WAKO Pure Chemical Industries Ltd (Osaka, Japan). Methyl 2-phenyl-propanoate (**6**), **3** and **4** were prepared by refluxing a MeOH solution of the corresponding acids in the presence of catalytic amounts of H_2SO_4.

2.2. Equipment

HPLC separations were achieved with a pump (PU-1580, JASCO, Tokyo, Japan), UV detector (UV-970M, JASCO, Tokyo, Japan), a manual injector (Rheodyne (IDEX Health & Science LLC, Tokyo, Japan), 20 μL loop), and a NaI(Tl) well-type scintillation detector with an ACE Mate Amplifier and BIAS supply (925-SCINT, ORTEC, Oak Ridge, TN, USA) for radioactivity detection. Data acquisition and interpretation were performed with EZChrom Elite (Scientific Software Inc., San Ramon, CA, USA). The enantiomeric purity (% ee) was measured by an analytical HPLC system with a pump (PU-2089 plus, JASCO, Tokyo, Japan) and the same radiodetector described

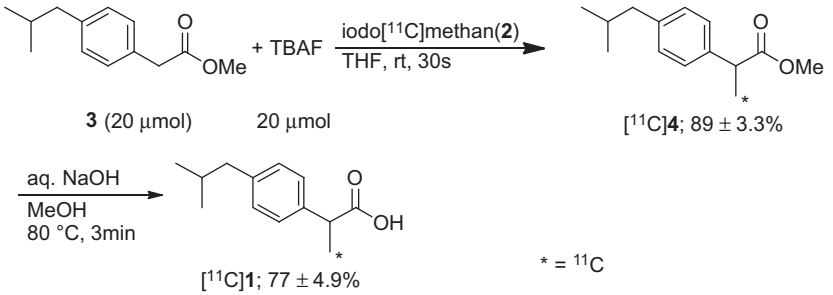

Scheme 1. Synthesis of [^{11}C]**1** via TBAF-promoted α-[^{11}C]methylation of **3** using **2** in THF.

above. The remote-controlled system for radiolabeling under high radioactivity level was composed in-house. Inversion of (*R*)-[^{11}C]**1** to (*S*)-[^{11}C]**1** in the blood of mice was quantified by the same HPLC system, except for the use of a high sensitive positron detector (Ohyo Koken Kogyo Co. Ltd, Tokyo, Japan).

PET scans of mice were performed with an Inveon Dedicated PET system (Siemens Medical Solutions, Knoxville, TN, USA). Mice were anesthetized with 2% isoflurane using a small animal anesthetizer (TK-6, Bio Machinery, Chiba, Japan), and the body temperature was maintained within the normal range using a heating pad system (Mul·T·Pads with T/Pump, Gaymar Industries Inc., Orchard Park, NY, USA) during the PET scans. The radioactivity was obtained with volume of interest (VOI) analysis using the ASI-Pro VM software (CTI Concorde Microsystems, Knoxville, TN, USA). The radioactivity of the injected solution and that in the plasma were measured with a dose calibrator (IGC-7, ALOKA, Tokyo, Japan).

2.3. Systems for HPLC

HPLC was performed using the following systems.

System A: Analytical HPLC of [^{11}C]**6** was performed with an analytical reversed-phase XBridge C18 column (150 × 4.6 mm, 3.5 μm, Waters Corporation, Milford, MA, USA). Elution was performed at a flow rate of 0.7 mL/min with MeCN/buffer/AcOH (60:40:0.2). A 30 mM solution of NH_4OAc was used for the buffer. UV absorption was detected at 254 nm.

System B: Analytical HPLC of [^{11}C]**4** was performed with an analytical reversed-phase XBridge C8 column (150 × 4.6 mm, 3.5 μm, Waters Corporation, Milford, MA, USA). Elution was performed at a flow rate of 0.7 mL/min with MeCN/buffer/AcOH (70:30:0.2). A 30 mM solution of NH_4OAc was used for the buffer. UV absorption was detected at 254 nm.

System C: Analytical HPLC of [^{11}C]**1** was performed with an analytical reversed-phase XBridge C18 column (150 × 4.6 mm, 3.5 μm, Waters Corporation, Milford, MA, USA). Elution was performed at a flow rate of 0.7 mL/min with MeCN/buffer/AcOH (60:40:0.2). A 30 mM solution of NH_4OAc was used for the buffer. UV absorption was detected at 254 nm.

System D: Preparative HPLC of [^{11}C]**1** was conducted with a semi-preparative reversed-phase CHIRALPAC OJ-RH column (150 × 20 mm, 5 μm, DAICEL Co. Ltd, Tokyo, Japan). Elution was performed at a flow rate of 7.5 mL/min with MeCN/buffer (45:55). A sodium phosphate solution (30 mM, pH 2.5) was used for the buffer. UV absorption was detected at 254 nm.

System E: The enantiomeric purity of isolated (*R*)- or (*S*)-[^{11}C]**1** were determined with an analytical reversed-phase CHIRALPAC OJ-RH column (150 × 4.6 mm, 5 μm, DAICEL Co. Ltd, Tokyo, Japan). Elution was performed at a flow rate of 0.5 mL/min with MeCN/buffer (50:50). A sodium phosphate solution (20 mM, pH 3) was used for the buffer. UV absorption was detected at 254 nm.

System F: The specific activities and the radiochemical purities of isolated (*R*)- or (*S*)-[^{11}C]**1** were determined with an analytical reversed-phase XBridge C18 column (50 × 3.0 mm, 2.5 μm, Waters Corporation, Milford, MA, USA). Elution was performed at a flow rate of 1 mL/min with 90% MeCN/buffer (60:40). A mixture of 100 mM of $(NH_4)_3PO_4$ (pH 2) and 5 mM of $C_8H_{17}SO_4Na$ was used for the buffer. UV absorption was detected at 254 nm.

2.4. Production of 2

[^{11}C]Carbon dioxide was produced by the $^{14}N(p,\alpha)^{11}C$ nuclear reaction in a nitrogen gas containing 0.01% oxygen with 18 MeV protons using the CYPRIS HM-18 cyclotron (Sumitomo Heavy Industry, Tokyo, Japan). After bombardment, [^{11}C]O_2 was transferred to the reaction vessel where a 0.05 M THF solution of LAH (500 μL) was placed at 0 °C. After evaporating THF, an aqueous 57% HI solution (400 μL) was added to the vessel. The resulting mixture was heated to 150 °C to produce iodo[^{11}C]methane (**2**). Gaseous **2** was transferred by a N_2 gas stream with a flow rate of 30 mL/min and collected by the reaction solvent (0.5–1 mL) in a glass vessel at room temperature (rt). The preparation time of **2** was around 7 min after the end of bombardment. The solution of **2** was divided into 100 μL aliquots and used for the α-[^{11}C]methylation reaction.

2.5. A typical procedure for the reaction yielding [^{11}C]6 in Table 1

A mixture of **5** (200 μL) and TBAF (1.0 M in THF) in a solvent (200 μL) was prepared a few minutes prior to the end of bombardment. A solution of **2** (37–370 MBq, 100 μL) was added to the mixture of **5** and TBAF and stored for 30 s at rt. Acetic acid (100 μL) was added to a reaction solution and the resulting mixture was analyzed by system A.

2.6. Synthesis of [^{11}C]1 by the low radioactivity level in THF

A mixture of **3** (20 μmol) in THF (200 μL) and TBAF (1.0 M in THF, 20 μL, 20 μmol) was prepared a few minutes prior to the end of bombardment. A solution of **2** (37−370 MBq) in THF (100 μL) was added to a mixture of **3** and TBAF and stored for 30 s at rt. To the reaction mixture, a mixture of MeOH (200 μL) and NaOH (1 M, 200 μL) was added and the resulting solution was heated at 80 °C. After 3 min, acetic acid (100 μL) was added to a reaction solution and the resulting mixture was analyzed by system C.

2.7. Synthesis of [^{11}C]1 under the low radioactivity level in DMSO

A mixture of solutions of **3** (10 μmol) in DMSO (200 μL) and TBAF (1.0 M in THF, 10 μL, 10 μmol) was prepared a few minutes prior to the end of bombardment. A solution of **2** (37−370 MBq) in DMSO (100 μL) was added to a mixture of **3** and TBAF and stored for 30 s at rt. For the analysis of **4**, the reaction mixture was quenched by the addition of acetic acid (100 μL) and analyzed by system B. To the unquenched reaction mixture, an aqueous solution of NaOH (1 M, 300 μL) was added and the resulting solution was heated at 60 °C. After 2 min, acetic acid (100 μL) was added to a reaction solution and the resulting mixture was analyzed by system C.

2.8. Synthesis of [^{11}C]1 under the high radioactivity level in DMSO

A mixture of solutions of **3** (10 μmol) in DMSO (300 μL) and TBAF (1.0 M in THF, 10 μL, 10 μmol) was prepared a few minutes prior to the end of bombardment and put into the reaction vessel. The ^{11}C-labeled agent **2** was prepared by the above method and transferred to the reaction vessel containing a solution of **3** and TBAF by a N_2 gas stream with a flow rate of 30 mL/min at rt. After the radioactivity of the vessel reached a plateau, the gas stream was suspended. After 30 s, an aqueous solution of NaOH (1 M, 300 μL) was added to the reaction mixture and then mixed by the N_2 gas stream. The mixture was heated to 60 °C and placed for 2 min at the same temperature. The reaction mixture was cooled by the air flow, flowed by the addition of a 9:1 mixture of eluent and H_3PO_4 (500 μL). Purification of (*R*)- or (*S*)-[^{11}C]**1** was carried out by system D. The desired individual isomers [^{11}C]**1** were collected by the flask containing a mixture of EtOH and Tween 80. The fraction was evaporated and the radioactive residue

was dissolved in an aqueous Na_2HPO_4 solution (50 mM, 2 mL) to neutralization. Enantiomeric purity and specific activity were determined by system E and system F, respectively.

2.9. PET measurements of (*R*)- and (*S*)-[^{11}C]1 accumulation in the joints of arthritis mice

Male mice (BALB/cCr Slc, 6–7 weeks old) used in the present study were purchased from Japan SLC Inc. (Shizuoka, Japan), and treated and handled according to the 'Recommendations for Handling of Laboratory Animals for Biomedical Research', compiled by the Committee on Safety and Ethical Handling Regulations for Laboratory Animal Experiments, National Institute of Radiological Sciences, Japan.

Anti-collagen antibody induced arthritis model mice were generated by intravenous injection of an arthritogenic monoclonal antibody cocktail (1.5 mg), consisting of five monoclonal anti-type II collagen antibodies (Arthrogen-CIA, Chondrex, Redmond, WA, USA) followed by the intraperitoneal injection of lipopolysaccharide (30 μg) on the third day following the administration of the antibody. At day 4, after the lipopolysaccharide injection, the mice, whose arthritis score of each limb was 3 according to the manufacturer's instructions, were used for PET examination as an arthritis model.

Eight normal mice and four arthritis model mice were used for PET scanning. The body temperature was maintained within the normal range using a heating pad system. The phosphate buffered solutions, which contained (*R*)- or (*S*)-[^{11}C]**1** at high concentrations, were diluted with saline to appropriate concentrations of radioactivity for the injection. Each of the (*R*)- and (*S*)-[^{11}C]**1** species (9 to 12 MBq; <0.18 nmol) were administered as a 0.2 mL intravenous bolus injection to each mouse. The mice were maintained under isoflurane anesthesia during the scanning periods. Data were acquired by the animal tomograph for 30 min following the injection in 13 frames divided as follows: 5 × 1 min, 5 × 2 min and 3 × 5 min frames. Without attenuation correction, the data were reconstructed using Fourier re-binning and filtered back projection with a Hanning filter cutoff at the Nyquist frequency into images with a 128 × 128 × 159 matrix size and twice zoom, to give a voxel size of 0.39 × 0.39 × 0.80 mm^3. After image reconstruction, VOI covering 3–4 slices were manually placed on a transverse view of summed PET images and transferred to all of the frames of the images to generate time–radioactivity concentration (Bq/mL) curves for heart and bilateral ankles. To compare the accumulation of the isomers to the joints of arthritis mice rigorously, PET scans of the isomers were performed with the same arthritis mouse on the same day. That is, an arthritis mouse was administrated (*R*)- or (*S*)-[^{11}C]**1** 5 h following the administration of the other isomer.

The statistical analysis of the time–activity curves was performed with the three-way ANOVA followed by the Holm-Sidak test using SigmaPlot (ver. 11, Systat Software Inc.). The significance level was set at p <0.01.

2.10. Determination of the component of radioactive compounds in the mice plasma after (*R*)- and (*S*)-[^{11}C]1 administration

After intravenous administration of (*R*)- and (*S*)-[^{11}C]**1** (70–125 MBq; <0.43 nmol) to normal mice (n = 3 each, 20–25 g), they were decapitated at 30 min. Blood samples (0.5 mL) were collected at the stump to a heparinized tube, and centrifuged at 10,000×g for 10 min to obtain the plasma. The plasma samples (0.2 mL) were mixed with a twofold volume of ethanol in a tube followed by centrifugation at 10,000×g for 5 min to deproteinize. The supernatant was filtered with a 0.45 μm pore membrane (Centricut W-MO, Kurabo Industries Ltd., Osaka, Japan), and the filtrate (50 μL) was subjected to HPLC analysis (system E). The recovery of the radioactivity in the filtrate was quantitatively based on the plasma radioactivity. The peaks of (*R*)- and (*S*)-[^{11}C]**1** on the radiochromatogram were confirmed by UV absorption of non-radioactive **1** coinjected to HPLC. The ratio of the components of the radioactive compounds was calculated after correcting the radiochromatogram for baseline noise and decay.

3. Results

3.1. Synthesis of [^{11}C]1 under low radioactivity level

The synthesis of [^{11}C]**1** should be carried out under the high radioactivity level. In our previous report, sufficient amounts of racemic [^{11}C]**1** was obtained when starting with ~11 GBq of [^{11}C]O_2. However, this synthesis approach was not used with a scale over 15 GBq, which was the standard level of radiolysis in a previous report.[11] No information about the radiolysis of [^{11}C]**4** with high radioactivity was available under the TBAF-mediated α-[^{11}C]methylation. However, similar radiolysis of [^{11}C]**4** was expected and such radiolysis would appear at the end of the α-[^{11}C]methylation of **3** and the beginning of the hydrolysis of [^{11}C]**4**. The addition of ascorbic acid, ethanol, or formic acid to the mixture after the reaction had been carried out was found to counter radiolysis; however, these treatments retard the TBAF-mediated [^{11}C]methylation process.[17] Ideally the most suitable approach would involve no addition of reagents to prevent radiolysis, but rely on the reaction solvent to suppress the radiolysis. Thus, we explored the possibility of using a different reaction solvent (other than THF) of the TBAF-mediated α-[^{11}C]methylation. The effect of the radiolysis of [^{11}C]**4** was investigated by analyzing the successive ester hydrolysis of [^{11}C]**4** without any additives.

Initially, the α-[^{11}C]methylation of **5** was chosen as a model reaction and explored in several solvents. All reactions in Table 1 were carried out by the addition of a solution of **2** to a mixture of **5** and TBAF at rt for 30 s. A mixture of **5** and TBAF was prepared about 10 min before the addition of a solution of **2**. As seen in Table 1, TBAF underwent α-[^{11}C]methylation efficiently in DMSO and the decay-corrected radiochemical conversion of **5** was more than 98%. The radiochemical conversion of [^{11}C]**6** was similar to that observed in THF (entries 1 and 2). In contrast to the reaction in THF, α-[^{11}C]methylation in DMSO led to a reduction in the amount of both precursor and TBAF while maintaining the radiochemical conversion of [^{11}C]**6** (entries 5–7). The reaction in acetonitrile was significantly less efficient and in dichloromethane was not effective under the ^{11}C-labeling conditions (entries 3 and 4).

We applied the conditions of entry 6 for the synthesis of [^{11}C]**1** under the small bombardment experiment. The [^{11}C]methylation of **3** in DMSO gave [^{11}C]**4** in 93 ± 1.2% radiochemical conversion (decay-corrected). The successive alkaline hydrolysis of the methyl

Table 1
TBAF-mediated α-[^{11}C]methylation of **5**[a]

Entry	Solvent	TBAF (μmol)	**5** (μmol)	RCC[b] (%)
1[c]	THF	20	20	95>
2	DMSO	20	20	98>
3	MeCN	20	20	13 ± 1.1
4	CH_2Cl_2	20	20	0
5	THF	10	10	61 ± 2.6
6	DMSO	10	10	95>
7	DMSO	5	5	91

[a] Each reaction was carried out more than three times.
[b] The radiochemical conversion (RCC) was determined by the radiochromatogram of the analytical HPLC following the decay correction.
[c] Ref.[11].

ester was carried out by the addition of an aqueous solution of NaOH to the reaction mixture and heated at 60 °C for 2 min. The reaction gave [^{11}C]**1** in 92 ± 2.8% radiochemical conversion (Scheme 2, in two steps, decay-corrected). The radiochemical conversions for both [^{11}C]**1** and [^{11}C]**4** were improved using the solvent DMSO and smaller starting amounts of TBAF and **3**, compared to the reaction with THF, were used (Schemes 1 and 2).

3.2. Synthesis of racemic [^{11}C]1 under high radioactivity level and its chiral separation

After successfully synthesizing racemic [^{11}C]**1** using DMSO under the low radioactivity level, we applied this method using DMSO for the efficient synthesis and chiral separation of [^{11}C]**1**. Our previous results using THF were not significantly different from DMSO and thus the synthesis using THF was also investigated. We performed the remote-controlled synthesis of [^{11}C]**1** and the radioactivity of [^{11}C]O_2 was scaled to >22.2 GBq (calculated amount). In both solvent conditions, α-[^{11}C]methylation was carried out by flowing gaseous nitrogen containing **2** into a solution of **3** at rt. Consequently, during the trapping of **2**, α-[^{11}C]methylation of **3** underwent simultaneously. The time-course radioactivity of the solution in the reaction vessel was monitored by a simple radioactivity sensor.[18]

In contrast to the synthesis under the low radioactivity level, low efficiency of radioactivity was observed for the trapping of **2** in THF. After the ester hydrolysis of [^{11}C]**4**, isolation of (*R*)- or (*S*)-[^{11}C]**1** using chiral HPLC was performed. In this case, significant amounts of radioactive hydrophilic byproducts were observed in the radiochromatogram (Fig. 1A). As a result of these negative factors, the radioactivity of the chiral product was less than 185 MBq (<1% decay uncorrected yield, referred to [^{11}C]O_2). On the other hand, the trapping efficiency of **2** during the α-[^{11}C]methylation in DMSO was consistent with the reaction carried out using 11.1 GBq of [^{11}C]O_2. Furthermore, the radiochromatogram of the reaction mixture following the ester hydrolysis of [^{11}C]**4** suggested significant suppression of the formation of hydrophilic byproducts (Fig. 1B). As a result, the obtained radioactivity of each isomer was more than 740 MBq (>3% decay uncorrected yield, referred to [^{11}C]O_2) and the range of specific activities was 66–289 GBq/μmol. The ees were more than 95% for the (*R*)-isomer and 90% for the (*S*)-isomer (Fig. 2). The radiochemical purity of injection solution of each isomer was always more than 99% even at the end of in vivo study.

The HPLC conditions for the separation of both isomers using chiral semi-preparative HPLC were determined as below. Since reversed-phase conditions are frequently introduced for PET tracer syntheses, the choice of a chiral column with a reversed-phase mode is preferable. We selected the Daicel OJ-RH column (20 × 150 mm, 5 μm) for preparative HPLC because this allowed us to use a mixture of MeCN and phosphate as an eluent without the addition of transition metal salts that require a further purification step.[19] Therefore, radioactive products will be administered only by adjusting the pH of the solution. Thus, chiral separation conditions for ibuprofen using semi-preparative HPLC were optimized by adjusting the flow rate and the ratio of MeCN and the buffer of the mobile phase. Optimum conditions that afforded efficient chiral separation for [^{11}C]**1** were a 45:55 mixture of MeCN and phosphate buffer as the eluent with a 7.5 mL flow rate (Fig. 1).

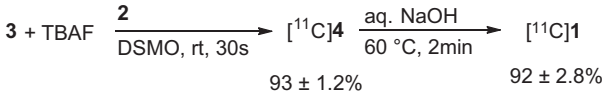

Scheme 2. Syntheses of [^{11}C]**1** under the low radioactive level.

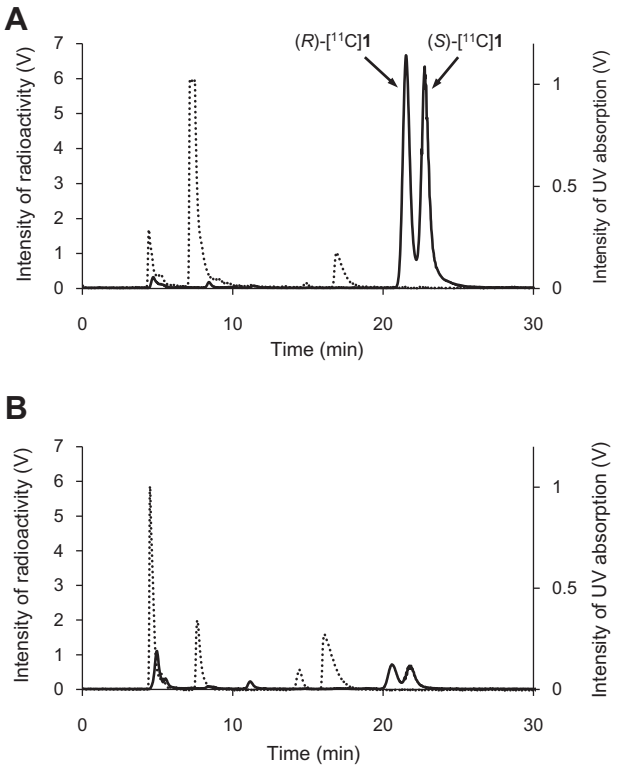

Figure 1. Radiochromatograms of preparative HPLC. Radiochromatogram (solid line) for the reaction mixture of the synthesis of [^{11}C]**1** via [^{11}C]methylation in DMSO (A) and in THF (B). The dotted lines represent the intensity of UV absorption at 254 nm.

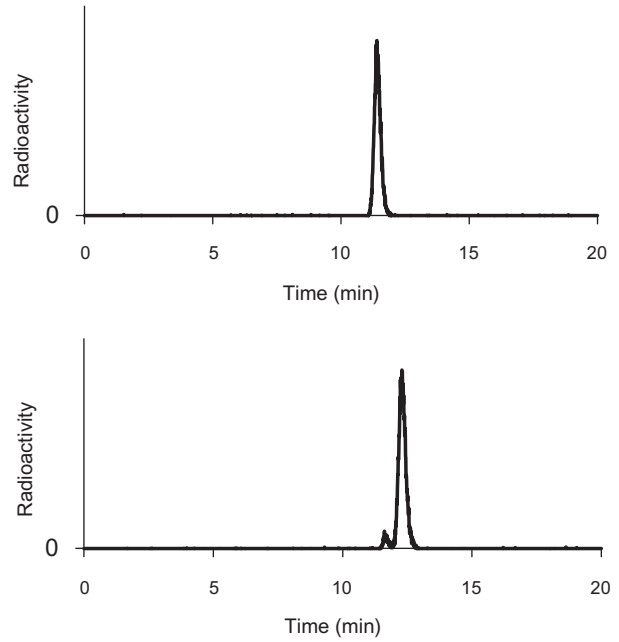

Figure 2. A typical radiochromatogram of isolated (*R*)- (upper) and (*S*)-[^{11}C]**1** (lower) after correcting for baseline noise and decay. The vertical axes (radioactivity) are presented as a relative value.

3.3. PET measurements of (*R*)- and (*S*)-[^{11}C]1 accumulation in the joints of arthritis mice

Since **1** has been used for the treatment of inflamed arthritis and anti-collagen antibody induced arthritis model mice represent

a well-established inflammation model, this model was used for investigating the accumulation of (*R*)- and (*S*)-[^{11}C]**1** at an inflamed lesion. PET scans of the isomers were performed with the same arthritis mouse for rigorous comparison of the accumulation of the isomers in the joints. PET images after the administration of the individual isomers to normal and arthritis mice are shown in Figure 3. In the PET images, the high accumulation of both isomers in the arthritic joints was observed. The concentration of radioactivity in the hindlimb ankles of mice almost reached a plateau during the 30 min of PET scanning (Fig. 4). The accumulation of the individual isomers in the hindlimb ankles of arthritis mice was more than twice as high as that of normal mice after 30 min post-injection (p <0.01). In contrast, comparable levels of the isomers accumulated in the ankles of arthritis and normal mice (not significant). The time–activity curves in the heart, which are considered to reflect the kinetics of radioactivity in the blood because of the high fraction binding of **1** to albumin,[20,21] were similar among all cases (not significant, Fig. 4). The uptake in other regions of normal mice such as cerebrum, liver, kidney and bladder were also similar between the isomers (Supplementary data).

3.4. Determination of the components of radioactive compounds in the plasma of mice after (*R*)- and (*S*)-[^{11}C]1 administration

(*R*)-**1** is inverted to the pharmacologically active (*S*)-isomer in terms of COX inhibition by 2-arylpropionyl-CoA epimerase in vivo.[22] Therefore, the concentration of (*R*)- and (*S*)-[^{11}C]**1** in plasma

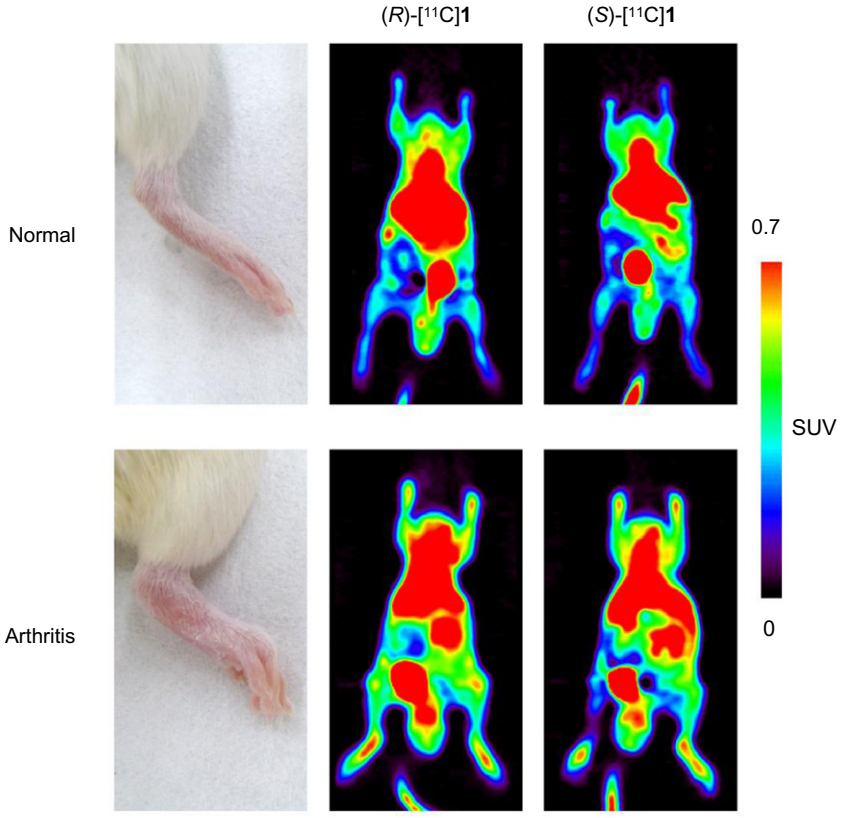

Figure 3. A typical swelling of the hindlimb of arthritic mice (left) and PET images after the administration of (*R*)- (center) and (*S*)-[^{11}C]**1** (right) to normal (upper) and arthritis mice (lower). Summed images during 0–30 min after the administration are presented.

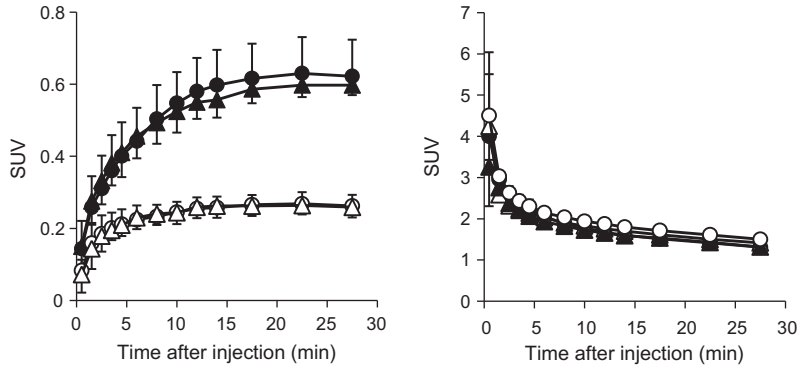

Figure 4. Time–activity curves of the ankle of the hindlimb (left) and the heart (right) after the administration of (*R*)- (circle) and (*S*)-[^{11}C]**1** (triangle) to normal (open) and arthritis mice (closed). The vertical axes represent the standardized uptake value (SUV: concentration of radioactivity in the VOI/(dose/body weight)).

Table 2
The fraction of components of radioactive compounds in the mice plasma after 30 min postinjection of the isomers

Injected isomer	Fraction of components (%)			
	Metabolites[a]	(*R*)-[^{11}C]**1**	(*S*)-[^{11}C]**1**	[^{11}C]**1**[b]
(*R*)-[^{11}C]**1**	25 ± 2.9	23 ± 4.3	52 ± 1.9	75 ± 2.9
(*S*)-[^{11}C]**1**	34 ± 2.8	0.78 ± 0.55	65 ± 3.2	66 ± 2.8

The values are expressed as mean ± SD (%, n = 3).
[a] The fraction of metabolites were calculated based on the whole radiochromatogram as shown in Figure 5, except for the regions of (*R*)- and (*S*)-[^{11}C]**1**.
[b] Sum of the (*R*)- and (*S*)-[^{11}C]**1**.

after the administration of the each isomer was determined. Following 30 min postinjection of (*R*)- and (*S*)-[^{11}C]**1** to normal mice, the concentration of radioactivity in the plasma was 8.3 ± 0.059% dose/mL and 8.9 ± 0.080% dose/mL, respectively. The ratio of components of radioactive compounds in the plasma following 30 min postinjection of the isomers is summarized in Table 2, and the chromatograms are presented in Figure 5. From the radioactivity and the ratio of components of [^{11}C]**1** in the plasma, the concentrations of [^{11}C]**1** (i.e., sum of (*R*)- and (*S*)-[^{11}C]**1**) in the plasma after 30 min postinjection of (*R*)- and (*S*)-[^{11}C]**1** were calculated as 5.9 ± 0.25% dose/mL and 6.2 ± 0.24% dose/mL, respectively.

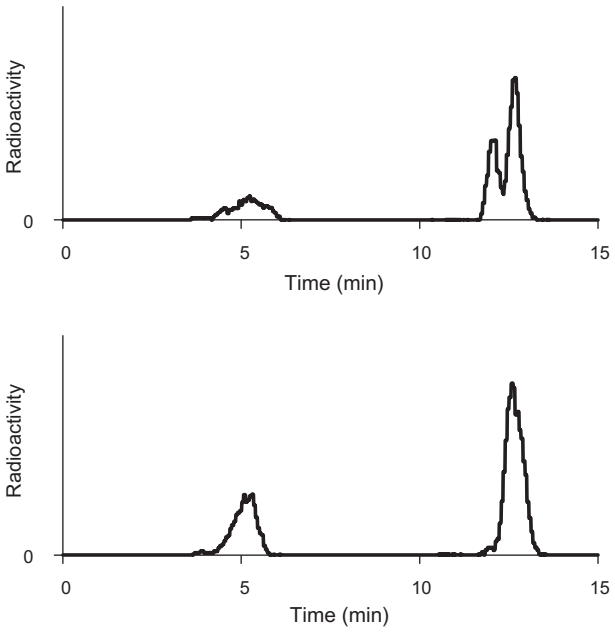

Figure 5. A typical radiochromatogram of radioactive compounds in the plasma after 30 min postinjection of (*R*)- (upper) and (*S*)-[^{11}C]**1** (lower) and following the correction for baseline noise and decay. The vertical axes (radioactivity) are presented as relative values.

4. Discussion

Higher order fluorides such as HF_2^-, $H_2F_3^-$ and additional ones were formed in the presence of water.[23] Those species were weaker bases than F^- and the reaction of **2** and **5** by tetrabutylammonium bifluoride did not undergo α-[^{11}C]methylation in either DMSO or THF. We considered that higher order fluorides could be formed from F^- in the presence of an acidic proton of **5** before the addition of a solution of **2**, and therefore retarded the production of the active anion of **5** (Eq. 1).[24] Additionally, different results on the α-[^{11}C]methylation by decreasing both TBAF and **5** in DMSO and THF were dominated by the reaction rate of the formation of higher order fluorides. These assumptions were supported by the result of α-[^{11}C]methylation of **5**, in which a high radiochemical conversion was maintained by changing the reaction manner. The reaction was carried out by the addition of 10 μmol of TBAF to a mixture of **2** and 10 μmol of **5** gave **6** with >95% radiochemical conversion (Eq. 2). The results were remarkably different from the radiochemical conversion of **6** obtained by the addition of **2** to a solution of 10 μmol of TABF and **5** (Table 1, entry 5). Therefore, the anion of **5** was generated sufficiently in the initial stages of the reaction and certain amounts of higher order fluorides were formed over the time course of the reaction in THF, thereby resulting in the slower α-[^{11}C]methylation of **5**. Similar observations were obtained by the α-[^{11}C]methylation of **5** in MeCN. The radiochemical conversion of **6** in MeCN gave rise to a dramatic increase to 72 ± 3.2% following the addition of TBAF to a mixture of **2** and **5** (Eq. 3). In contrast, the efficient α-[^{11}C]methylation of **6** occurred in the presence of smaller amounts of **5** and TBAF in DMSO. We concluded that the slower conversion of fluoride to higher order fluorides in DMSO consistently furnishes the sufficient active anion of **5**.

$$Bu_4NF + ArCH_2CO_2Me \rightleftharpoons Bu_4N^+ + ArCH^-CO_2Me + HF \xrightleftharpoons{Bu_4NF} Bu_4NHF_2 \quad (1)$$

$$[^{11}C]H_3I + \underset{\mathbf{2}}{\mathbf{5}} \xrightarrow[THF,\ rt,\ 30\ s]{TBAF} [^{11}C]\mathbf{6} \quad <95\% \quad (2)$$

$$\mathbf{2} + \mathbf{5} \xrightarrow[MeCN,\ rt,\ 30\ s]{TBAF} [^{11}C]\mathbf{6} \quad 72 \pm 3.2\% \quad (3)$$

The results of the synthesis of [^{11}C]**1** under the high radioactivity level differed remarkably between DMSO and THF. In contrast to unsuccessful results in THF, the efficient trapping of radioactivity under the preparation of [^{11}C]**4** and high yield of [^{11}C]**1** were acquired even by reducing the amount of **3** in DMSO. According to a former report, [^{11}C]**4** was labile but [^{11}C]**1** was resistant to the radiolysis.[10] Hydrophilic byproducts (ca. 25%) were observed in the reaction mixture of α-[^{11}C]methylation of **3** in THF under the high radioactivity level. The amounts of those products were insignificant under the low radioactivity level. We therefore consider that the different results in this study were derived from the radiolysis of the ester form [^{11}C]**4** and the primary role of DMSO was the suppression of this radiolysis.

Many groups have explored the scavenging effect of DMSO for hydroxyl radicals induced by γ-radiolysis, pulse radiolysis, the Fenton reaction and photolysis, and reaction pathways have been elucidated (Scheme 3).[25] TBAF used in this synthesis was a commercially available TBAF·3H_2O solution and the preparation

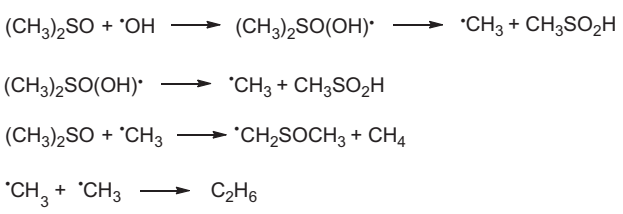

Scheme 3. Reaction pathways of DMSO and hydroxyl radicals.

of the reaction solutions were carried out under atmospheric conditions. Therefore, hydroxyl radicals could be formed under the α-[^{11}C]methylation condition of **3**; however, such radicals should be formed to a much lower level. On the other hand, **1** is considered to play a role as a radical scavenger or as an anti-oxidant to protect against oxidation of biogenic substances.[26] In addition, the presence of ibuprofen radicals under oxidative conditions was reported by spin trapping experiments.[5] Recently, von Gunten et al. reported the rate constant for the reaction of **1** and hydroxyl radicals.[27] They described that most of the products obtained by the reaction with hydroxyl radicals were phenolic compounds; however, structural information was not presented.[28] As compared to their reports, the expected concentrations of hydroxyl radicals in our conditions were lower. Thus, [^{11}C]**1** was also reactive against hydroxyl radicals; however, the radiolysis of [^{11}C]**1** was insignificant in this study. We summarized these results as follows. The radiolysis of [^{11}C]**4** was promoted by the presence of hydroxyl radicals, and the ester form [^{11}C]**4** was more reactive to these radicals than the acid form [^{11}C]**1**. The solvent effect by DMSO was effective in suppressing this type of radiolysis.

Finding an expedient system for HPLC separation of distinct substrates is necessary in PET tracer syntheses. Reversed-phase preparative HPLC was selected as the appropriate method to purify PET tracers. In contrast, chiral separation is usually performed using normal phase under non-labeling conditions. The use of a normal phase is technically burdensome because tedious replacement of the solution in the synthetic module should be carried out before and after every synthesis. In contrast, the buffer system used for reversed-phase chiral separation frequently contains perchrolate or copper ions. These conditions are also not preferable to PET tracer syntheses, because further treatments are required to remove those ions before administration.[15] Chiral separation by a regularly used buffer system such as phosphate or acetate was necessary and we explored HPLC conditions using a mixture of MeCN and sodium phosphate. Finally, we achieved an acceptable resolution for the preparation of individual isomers of [^{11}C]**1** and the isolated fraction could be administered by adjusting the pH with the addition of basic phosphate buffer.

The efficient synthesis of [^{11}C]**1** allowed sufficient preparation of (*R*)- and (*S*)-[^{11}C]**1** for the investigation of the in vivo kinetics of each isomer by PET. We investigated the accumulation of the individual stereo-isomer of [^{11}C]**1** in the joints of arthritis mice using PET as a preliminary experiment. The (*S*)-**1** isomer is known to inhibit COX activity, whereas the (*R*)-**1** is inactive.[1] Therefore, if COXs were involved in the accumulation of [^{11}C]**1** in the arthritic joints, the uptake of the (*S*)-isomer in the lesion would be higher than that of the (*R*)-isomer. However, the different accumulation levels of each isomer in the joints were not observed in both normal and arthritis mice throughout entire time course of the study. The (*R*)-[^{11}C]**1** remained in the plasma at the end of the PET scan and the kinetics of each isomer in the plasma was comparable. Consequently, the accumulation mechanism of [^{11}C]**1** in the arthritic lesions was considered to be independent of COX expression in the joints. This result was consistent with a previous report; Cox et al. reported that the steady-state distribution of isomers of **1** into synovial fluid is modulated by the binding of the isomers to albumin and the serum-synovial fluid albumin ratio.[29] Furthermore, increased blood flow in the arthritic lesion[30] and/or elimination of albumin, which is a carrier of **1**,[20] from the blood to the arthritic lesion[31] may be involved in the high accumulation of [^{11}C]**1** in the lesion. Although the accumulation mechanism of [^{11}C]**1** in the arthritic lesions remains to be investigated, our results suggest that [^{11}C]**1** or its chiral isomers can be used to detect arthritis in vivo. Recently, administration of (*S*)-**1** for pain relief rather than racemic **1** use[32] and drug–drug interactions between **1** and concomitant medicines such as methotrexate[33] were studied. [^{11}C]**1** or its chiral isomers can also be useful for those pharmacokinetic studies.

5. Conclusion

Efficient production of [^{11}C]**1** was realized via TBAF-mediated α-[^{11}C]methylation of **3** in DMSO. The solvent effects of DMSO for the suppression of radiolysis of [^{11}C]**4** and the behavior of the fluoride anion were remarkable. Individual isomers (*R*)-[^{11}C]**1** and (*S*)-[^{11}C]**1** were obtained by chiral separation using reversed-phase HPLC with high ee. The PET studies of individual isomers represent opportunities to investigate profens, including **1**, in more detail by molecular imaging technologies.

Acknowledgements

We thank the technical team of the Cyclotron Section and Radiopharmaceuticals Section of the National Institute of Radiological Sciences for their support during cyclotron operation and the production of radioisotopes. This work was supported in part by The Nakatomi Foundation and an Intramural Research Grant from the National Institute of Radiological Sciences.

Supplementary data

Supplementary data associated with this article can be found, in the online version, at doi:10.1016/j.bmc.2011.03.041.

References and notes

1. Adams, S. S.; Bresloff, P.; Mason, C. G. *J. Pharm. Pharmacol.* **1976**, *28*, 256.
2. Shen, T. Y. *Angew. Chem., Int. Ed. Engl.* **1972**, *11*, 460.
3. (a) Tegeder, I.; Pfeilschifter, J.; Geisslinger, G. *FASEB J.* **2001**, *15*, 2057; (b) Weggen, S.; Eriksen, J. L.; Das, P.; Sagi, S. A.; Wang, R.; Pietrzik, C. U.; Findlay, K. A.; Smith, T. E.; Murphy, M. P.; Bulter, T.; Kang, D. E.; Marquez-Sterling, N.; Golde, T. E.; Koo, E. H. *Nature* **2001**, *414*, 212; (c) Zhou, Y.; Su, Y.; Li, B.; Liu, F.; Ryder, J. W.; Wu, X.; Gonzalez-DeWhitt, P. A.; Gelfanova, V.; Hale, J. E.; May, P. C.; Paul, S. M.; Ni, B. *Science* **2003**, *302*, 1215.
4. Quann, E. J.; Khwaja, F.; Zavitz, K. H.; Djakiew, D. *Cancer Res.* **2007**, *67*, 3254.
5. Hamburger, S. A.; McCay, P. B. *Free Radical Res. Commun.* **1990**, *9*, 337.
6. Jedlitschky, G.; Tirschmann, K.; Lubenow, L. E.; Nieuwenhuis, H. K.; Akkerman, J. W. N.; Greinacher, A.; Kroemer, H. K. *Blood* **2004**, *104*, 3603.
7. (a) Fornasini, G.; Monti, N.; Brogin, G.; Gallina, M.; Eandi, M.; Persiani, S.; Bani, M.; Della Pepa, C.; Zara, G.; Strolin Benedetti, M. *Chirality* **1997**, *9*, 297; (b) Li, C.; Benet, L. Z.; Grillo, M. P. *Chem. Res. Toxicol.* **2002**, *15*, 1480; (c) Zheng, C.; Hao, H.; Wang, G.; Sang, G.; Sun, J.; Li, P.; Li, J. *Eur. J. Drug Metab. Pharmacokinet.* **2008**, *33*, 45.
8. Phelps, M. E. *Proc. Natl. Acad. Sci. U.S.A.* **2000**, *97*, 9226.
9. Lappin, G. R. C. *Garner, Nat. Rev. Drug Disc.* **2003**, *2*, 233.
10. Takashima-Hirano, M.; Shukuri, M.; Takashima, T.; Goto, M.; Wada, Y.; Watanabe, Y.; Onoe, H.; Doi, H.; Suzuki, M. *Chemistry* **2010**, *16*, 4250.
11. Kato, K.; Kikuchi, T.; Nengaki, N.; Arai, T.; Zhang, M.-R. *Tetrahedron Lett.* **2010**, *51*, 5908.
12. (a) Oppolzer, W.; Rosset, S.; De Brabander, J. *Tetrahedron Lett.* **1997**, *38*, 1539; (b) Noyori, R. *Angew. Chem., Int. Ed.* **2002**, *41*, 2008; (c) Knowles, W. S. *Angew. Chem., Int. Ed.* **2002**, *41*, 1999; (d) Goossen, L. J. *Angew. Chem., Int. Ed.* **2002**, *41*, 3775; (e) Alper, H.; Hamel, N. *J. Am. Chem. Soc.* **1990**, *112*, 2803; (f) Uemura, T.; Zhang, X.; Matsumura, K.; Sayo, N.; Kumobayashi, H.; Ohta, T.; Nozaki, K.; Takaya, H. *J. Org. Chem.* **1996**, *61*, 5510; (g) Chen, A.; Ren, L.; Crudden, C. M. *J. Org. Chem.* **1999**, *64*, 9704; (h) Li, X.; List, B. *Chem. Commun.* **2007**, 1739; (i) Smith, C. R.; RajanBabu, T. V. *Org. Lett.* **2008**, *10*, 1657; (j) Friest, J. A.; Maezato, Y.; Broussy, S.; Blum, P.; Berkowitz, D. B. *J. Am. Chem. Soc.* **2010**, *132*, 5930; (k) Fadel, A. *Synlett* **1992**, 48.

13. Zhang, Y.; Hong, Y.; Huang, C. C.; Belmont, D. *J. Labelled Compd. Radiopharm.* **2006**, *49*, 237.
14. Maier, N. M.; Franco, P.; Lindner, W. *J. Chromatogr., A* **2001**, *906*, 3.
15. Drandarov, K.; Schubiger, P. A.; Westera, G. *Appl. Radiat. Isot.* **2006**, *64*, 1613.
16. (a) MacGregor, R. R.; Schlyer, D. J.; Fowler, J. S.; Wolf, A. P.; Shiue, C. Y. *J. Nucl. Med.* **1987**, *28*, 60; (b) Scott, P. J.; Hockley, B. G.; Kung, H. F.; Manchanda, R.; Zhang, W.; Kilbourn, M. R. *Appl. Radiat. Isot.* **2009**, *67*, 88.
17. (a) Fukumura, T.; Nakao, R.; Yamaguchi, M.; Suzuki, K. *Appl. Radiat. Isot.* **2004**, *61*, 1279; (b) Fawdry, R. M. *Appl. Radiat. Isot.* **2007**, *65*, 1193; (c) Jacobson, M. S.; Dankwart, H. R.; Mahoney, D. W. *Appl. Radiat. Isot.* **2009**, *67*, 990.
18. Due to the high background radioactivity, precise measuring of radioactivity by simple sensor was difficult.
19. The web site of DAICEL CHEMICAL INDUSTRY Ltd shows the chiral separation data. See http://www.daicelchiral.com/appguide/index.htm. Their service section informed us the chiral separation of ibuprofen using CHIRALCEL OJ-RH by analytical scale.
20. (a) Itoh, T.; Maruyama, J.; Tsuda, Y.; Yamada, H. *Chirality* **1997**, *9*, 354; (b) Itoh, T.; Saura, Y.; Tsuda, Y.; Yamada, H. *Chirality* **1997**, *9*, 643.
21. Subramanian, K. M. *J. Nucl. Med.* **1991**, *32*, 480.
22. Reichel, C.; Brugger, R.; Bang, H.; Geisslinger, G.; Brune, K. *Mol. Pharmacol.* **1997**, *51*, 576.
23. Sun, H.; DiMagno, S. G. *J. Am. Chem. Soc.* **2005**, *127*, 2050.
24. Adams, D. J.; Clark, J. H.; Nightingale, D. J. *Tetrahedron* **1999**, *55*, 7725.
25. (a) Veltwisch, D.; Janata, E.; Asmus, K.-D. *J. Chem. Soc., Perkin Trans. 2* **1980**, 146; (b) Eberhardt, M. K.; Colina, R. *J. Org. Chem.* **1988**, *53*, 1071; (c) Woodward, J. R.; Lin, T.-S.; Sakaguchi, Y.; Hayashi, H. *J. Phys. Chem. A* **2000**, *104*, 557; (d) Koulkes-Pujo, A. M.; Barat, F.; Mialocq, J. C.; Sutton, J. *J. Photochem.* **1973/74**, *2*, 439.
26. Zapolska-Downar, D.; Zapolska-Downar, A.; Bukowska, H.; Gałka, H.; Naruszewicz, M. *Life Sci.* **1999**, *65*, 2289.
27. Huber, M. M.; Canonica, S.; Park, G. Y.; von Gunten, U. *Environ. Sci. Technol.* **2003**, *37*, 1016.
28. (a) von Gunten, U. *Water Res.* **2003**, *37*, 1443; (b) Pan, X.-M.; Schuchmann, M. N.; von Sonntag, C. *J. Chem. Soc., Perkin Trans. 2* **1993**, 289; (c) Mvula, E.; Schuchmann, M. N.; von Sonntag, C. *J. Chem. Soc., Perkin Trans. 2* **2001**, 264.
29. Cox, S. R.; Gall, E. P.; Forbes, K. K.; Gresham, M.; Goris, G. *J. Clin. Pharmacol.* **1991**, *31*, 88.
30. Clavel, G.; Marchiol-Fournigault, C.; Renault, G.; Boissier, M. C.; Fradelizi, D.; Bessis, N. *Ann. Rheum. Dis.* **2008**, *67*, 1765.
31. Wunder, A.; Müller-Ladner, U.; Stelzer, E. H.; Funk, J.; Neumann, E.; Stehle, G.; Pap, T.; Sinn, H.; Gay, S.; Fiehn, C. *J. Immunol.* **2003**, *170*, 4793.
32. (a) Kaehler, S. T.; Phleps, W.; Hesse, E. *Inflammopharmacology* **2003**, *11*, 371; (b) Moore, R. A.; Derry, S.; McQuay, H. J. *Cochrane Database Syst. Rev.* **2009**, *23*, 12.
33. El-Sheikh, A. A. K.; van den Heuvel, J. J. M. W.; Koenderink, J. B.; Russel, F. G. M. *J. Pharmacol. Exp. Ther.* **2007**, *320*, 229.